N-Glycans on EGF domain-specific *O*-GlcNAc transferase (EOGT) facilitate EOGT maturation and peripheral endoplasmic reticulum localization

Received for publication, December 11, 2019, and in revised form, April 30, 2020 Published, Papers in Press, May 6, 2020, DOI 10.1074/jbc.RA119.012280

Sayad Md. Didarul Alam[1], Yohei Tsukamoto[1,‡], Mitsutaka Ogawa[1,‡], Yuya Senoo[1], Kazutaka Ikeda[1,2], Yuko Tashima[1], Hideyuki Takeuchi[1], and Tetsuya Okajima[1,*]

From the [1]Department of Molecular Biochemistry, Nagoya University Graduate School of Medicine, Nagoya, Japan and [2]RIKEN, Center for Integrative Medical Sciences, Suehiro-cho, Tsurumi, Yokohama, Japan

Edited by Gerald W. Hart

Epidermal growth factor (EGF) domain-specific *O*-GlcNAc transferase (EOGT) is an endoplasmic reticulum (ER)-resident protein that modifies EGF repeats of Notch receptors and thereby regulates Delta-like ligand-mediated Notch signaling. Several *EOGT* mutations that may affect putative *N*-glycosylation consensus sites are recorded in the cancer database, but the presence and function of *N*-glycans in EOGT have not yet been characterized. Here, we identified *N*-glycosylation sites in mouse EOGT and elucidated their molecular functions. Three predicted *N*-glycosylation consensus sequences on EOGT are highly conserved among mammalian species. Within these sites, we found that Asn-263 and Asn-354, but not Asn-493, are modified with *N*-glycans. Lectin blotting, endoglycosidase H digestion, and MS analysis revealed that both residues are modified with oligomannose *N*-glycans. Loss of an individual *N*-glycan on EOGT did not affect its endoplasmic reticulum (ER) localization, enzyme activity, and ability to *O*-GlcNAcylate Notch1 in HEK293T cells. However, simultaneous substitution of both *N*-glycosylation sites affected both EOGT maturation and expression levels without an apparent change in enzymatic activity, suggesting that *N*-glycosylation at a single site is sufficient for EOGT maturation and expression. Accordingly, a decrease in *O*-GlcNAc stoichiometry was observed in Notch1 co-expressed with an N263Q/N354Q variant compared with WT EOGT. Moreover, the N263Q/N354Q variant exhibited altered subcellular distribution within the ER in HEK293T cells, indicating that *N*-glycosylation of EOGT is required for its ER localization at the cell periphery. These results suggest critical roles of *N*-glycans in sustaining *O*-GlcNAc transferase function both by maintaining EOGT levels and by ensuring its proper subcellular localization in the ER.

Epidermal growth factor-like (EGF) domain-specific *O*-GlcNAc transferase (EOGT) is a luminal endoplasmic reticulum (ER) protein that modifies Ser/Thr residues conserved on a subset of EGF domains of secreted and transmembrane proteins (1–3). Unlike OGT-mediated regulation of *O*-GlcNAcylated cytoplasmic, mitochondrial, and nuclear proteins, EOGT can modulate pericellular protein function directly by extracellular *O*-GlcNAc modifications of transmembrane or secreted proteins (4). The biological significance of extracellular *O*-GlcNAc is further suggested by *EOGT* mutations found in patients with Adams-Oliver syndrome, a rare disorder characterized by congenital limb abnormalities and scalp defects (5, 6).

Genomic analysis of *EOGT* in Adams-Oliver syndrome patients revealed several missense and nonsense mutations, including W206S, R377Q, and 359Dfs*28, all of which result in the loss of enzyme activity (7). In somatic cancer mutation databases, additional missense and nonsense mutations have been registered, although their functional consequences have not been addressed. Of particular interest are *EOGT* mutations at putative *N*-glycosylation sites. It was recently shown that *N*-acetylglucosaminyltransferase III/Mgat3-mediated bisecting of *N*-glycans regulates Notch1 function by changing Notch1 subcellular localization (8). However, the significance of *N*-glycans on Notch-modifying enzymes has not been extensively studied. Bovine *O*-fucosyltransferase 1 (POFUT1), another EGF-domain specific ER enzyme (9), possesses two *N*-glycans (10, 11) that are required for its enzyme activity and solubility. However, the effect of POFUT1 *N*-glycans on its enzymatic products has not addressed directly yet and needs further investigation.

In this study, we characterized mouse EOGT to determine all *N*-glycosylation sites, detailed *N*-glycan structures, and their effect on EOGT expression, localization, and enzymatic function. *N*-Glycans on EOGT impacted protein maturation and *O*-GlcNAc stoichiometry, although a single *N*-glycan was sufficient to mediate these functions. Importantly, our results provided the first evidence of ER-resident proteins whose *N*-glycans facilitate their distribution to the peripheral ER.

Results

EOGT is modified with N-glycans

EOGT is an ER-resident protein with an N-terminal signal peptide and C-terminal KDEL-like motif that acts as an ER retrieval signal for secreted proteins (Fig. 1*A*) (2). The predicted *N*-glycosylation sites on EOGT are located in highly conserved regions in various mammalian species including *Mus musculus* (mouse), *Rattus norvegicus* (Norway rat), *Oryctolagus cuniculus* (rabbit), *Bos taurus* (cow), *Sus scrofa* (wild pig), *Homo sapiens* (human), and *Canis lupus familiaris* (dog) (Fig. 1*B*). Mouse

This article contains supporting information.
‡These authors contributed equally to this work.
* For correspondence: Tetsuya Okajima, tokajima@med.nagoya-u.ac.jp.

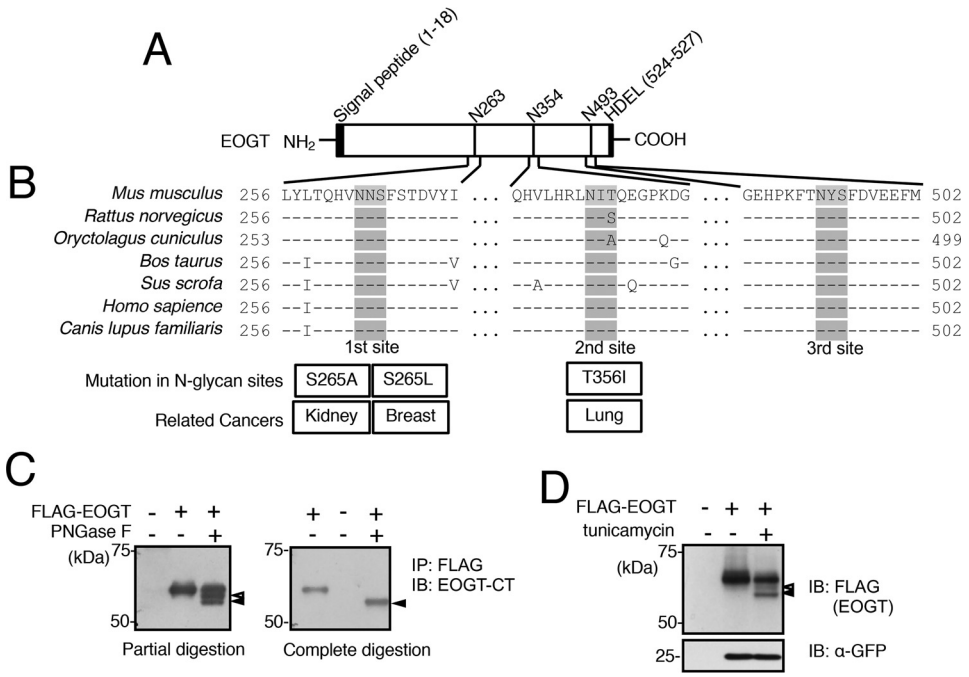

Figure 1. EOGT is modified with *N*-glycans. *A*, schematic representation of mouse EOGT structure. Three *N*-glycosylation sequons, the N-terminal signal peptide, and the KDEL-like ER retention signal are indicated. *B*, multiple alignment of amino acid sequences from seven mammalian EOGT. Amino acid sequences and amino acid numbers surrounding the putative *N*-glycosylation sites are shown. The conserved *N*-glycosylation sites are highlighted by *gray boxes*. The amino acid residues identical to mouse EOGT are indicated by *dashes*. Three *EOGT* mutations found in the cancer database are also indicated. *C*, FLAG-EOGT was expressed in HEK293T cells and immunoprecipitated from the cell lysates by FLAG antibody. FLAG-EOGT was incubated with PNGase F to partially (*left*) or completely (*right*) remove *N*-glycans. EOGT-CT antibody was used for immunoblotting to detect the full-length form of EOGT. Partially or completely digested products are indicated by *open* or *closed arrowheads*, respectively. *D, Eogt*-transfected HEK293T cells were treated with or without tunicamycin for 24 h, and cell lysates were analyzed by immunoblotting using FLAG and GFP antibodies. Immunoblot bands corresponding to partially or completely deglycosylated products are indicated by *open* or *closed arrowheads*, respectively. GFP bands show similar transfection efficiency in the samples.

EOGT contains three N-*X*-S/T (X ≠P) sequons for *N*-linked glycosylation at Asn-263, Asn-354, and Asn-493. The first and third *N*-glycosylation sequons are exclusively conserved in these mammals. The second sequon is not fully conserved as seen in the case of *O. cuniculus*, where only two *N*-glycosylation sites were found. Except for *S. scrofa*, where one additional site (Ans-141) is present, no other sequons were present on EOGT. The ICGC cancer database registered several somatic mutations affecting two *N*-glycosylation sequons (S265A, S265L, and T356I), and some of them are classified as potentially pathogenic (Fig. 1*B*). However, there was no evidence that these Asn residues are modified with *N*-glycans and have a general role in EOGT function, since no functional analysis had been performed.

To analyze *N*-glycans on EOGT, mouse FLAG-EOGT was heterologously expressed in HEK293T cells and affinity-purified from cell lysates. To detect the intact full-length form of FLAG-EOGT, we raised the carboxyl-terminal EOGT (EOGT-CT) antibody. As expected, this antibody hardly detects the deletion mutant lacking four amino acids from the end of the C terminus of FLAG-EOGT (Fig. S1). FLAG- EOGT was transgenically expressed and detected by using the FLAG antibody for immunoprecipitation and the EOGT-CT antibody for immunoblotting. Partial removal of *N*-glycans from FLAG-EOGT with PNGase F produced two faster-migrating bands, and the lower band corresponded to the band generated after complete digestion, suggesting the presence of at least two *N*-glycans on EOGT (Fig. 1*C*). To confirm the *in vitro* results, *Eogt*-transfected HEK293T cells were treated with tunicamycin, a potent inhibitor of GlcNAc phosphotransferase that is involved in the synthesis of lipid-linked *N*-glycan precursors. Immunoblotting with the FLAG antibody recapitulated the band shifts caused by the loss of *N*-glycans on EOGT (Fig. 1*D*). These results demonstrated the presence of multiple *N*-glycans on mouse EOGT.

Identification of two N-glycans sites on mouse EOGT

To identify which *N*-glycosylation sequons on EOGT are occupied with *N*-glycans, three *Eogt* mutants were generated by site-directed mutagenesis where asparagine was replaced by glutamine (Fig. 2*A*). The N263Q and N354Q EOGT isoforms expressed in HEK293T cells, but not the N493Q mutant, showed decreased molecular weight. These data show that the former two sites are modified with *N*-glycans (Fig. 2*B*).

To prove the presence of two *N*-glycosylation sites on EOGT, each FLAG-EOGT isoform was partially digested with PNGase F. Both the N263Q and N354Q mutants showed one additional band, whereas the N263Q/N354Q double mutant did not change its apparent molecular weight on the gels (Fig. 2*B*). Similar results were obtained in the transfected cells treated with or without tunicamycin (Fig. 2*C*). These results demonstrated that mouse EOGT is modified with *N*-glycans at the Asn-263 and Asn-354 sites. The lack of *N*-glycans in the N263Q/N354Q mutant indicated that there was no compensatory gain of glycosylation at the Asn-493 site in the absence of the Asn-263 and Asn-354 sites.

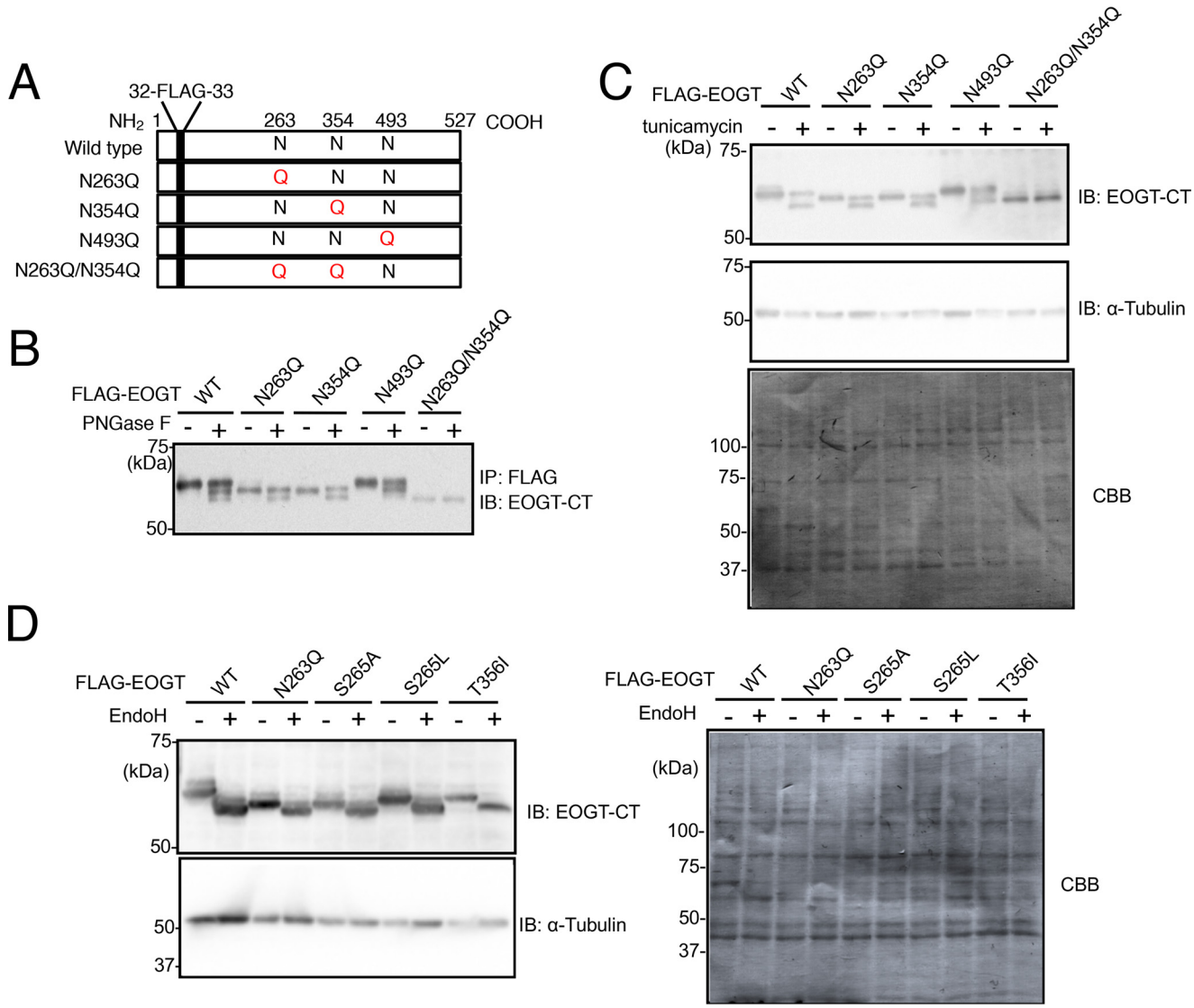

Figure 2. Identification of two *N*-glycosylation sites on mouse EOGT. *A*, schematic representation showing the generation of FLAG-EOGT variants containing *N*-glycosylation site mutations. Asparagine (*N*) residues were replaced with glutamine (*Q*) residues. *B*, each FLAG-EOGT isoform was expressed in HEK293T cells and immunoprecipitated by FLAG antibody. FLAG-EOGT was incubated with PNGase F to partially remove *N*-glycans. EOGT-CT antibody was used to detect full-length EOGT. *C*, HEK293T cells were transfected to express each FLAG-EOGT isoform and treated with or without tunicamycin for 48 h. Cell lysates were analyzed by immunoblotting with EOGT-CT and α-tubulin antibodies. After immunoblotting, the PVDF membrane was stained with Coomassie Brilliant Blue (*CBB*) as the protein loading control. *D*, FLAG-EOGT harboring cancer-related mutations (S265A, S265L, and T356I) were expressed in HEK293T cells and treated with or without Endo H. WT and N263Q FLAG-EOGT were analyzed in parallel as controls. After immunoblotting with EOGT-CT and α-tubulin antibodies, the PVDF membrane was stained with Coomassie Brilliant Blue as the protein loading control.

To examine the effect of cancer-related mutations found in these *N*-glycosylation sequons, a FLAG-EOGT protein harboring S265A, S265L, or T356I mutation was analyzed in parallel with the WT and N263Q FLAG-EOGT proteins. All of the cancer-related mutants showed electrophoretic mobility similar to that of the N263Q mutant regardless of the deglycosylation by Endo H treatment. These data demonstrated that the S265A, S265L, or T356I mutations result in a single *N*-glycan modification on EOGT (Fig. 2*D*).

EOGT is modified with oligomannose N-glycans

To characterize the *N*-glycan structure on EOGT, lectin blotting was performed using concanavalin A (ConA), a lectin that binds tightly oligomannose-type and hybrid-type *N*-glycans. As expected from their ER localization, EOGT and the N263Q or N354Q mutants were readily detectable with ConA, whereas the N263Q/N354Q double mutant was no longer bound (Fig. 3*A*).

To determine the *N*-glycan structures on EOGT, purified FLAG-EOGT was subjected to tryptic or chymotryptic digestion followed by LC–MS analysis. MS/MS spectra showed that LTQHVN^{263}NSFSTDVY and LN^{354}ITQEGPK peptides are modified with oligomannose *N*-glycans (Fig. 3*B*). Semiquantitative analysis revealed that the HexNAc2Hex9 and HexNAc2Hex8 glycoforms are predominant on the Asn-263 site, whereas the HexNAc2Hex8 and HexNAc2Hex7 glycans are relatively abundant on the Asn-354 site. A fraction of oligomannose *N*-glycans exhibit HexNAc2Hex6 and HexNAc2Hex5 glycoforms (Fig. 3*C*). However, only a few are further processed to HexNAc4Hex3dHex complex *N*-glycans consistent with

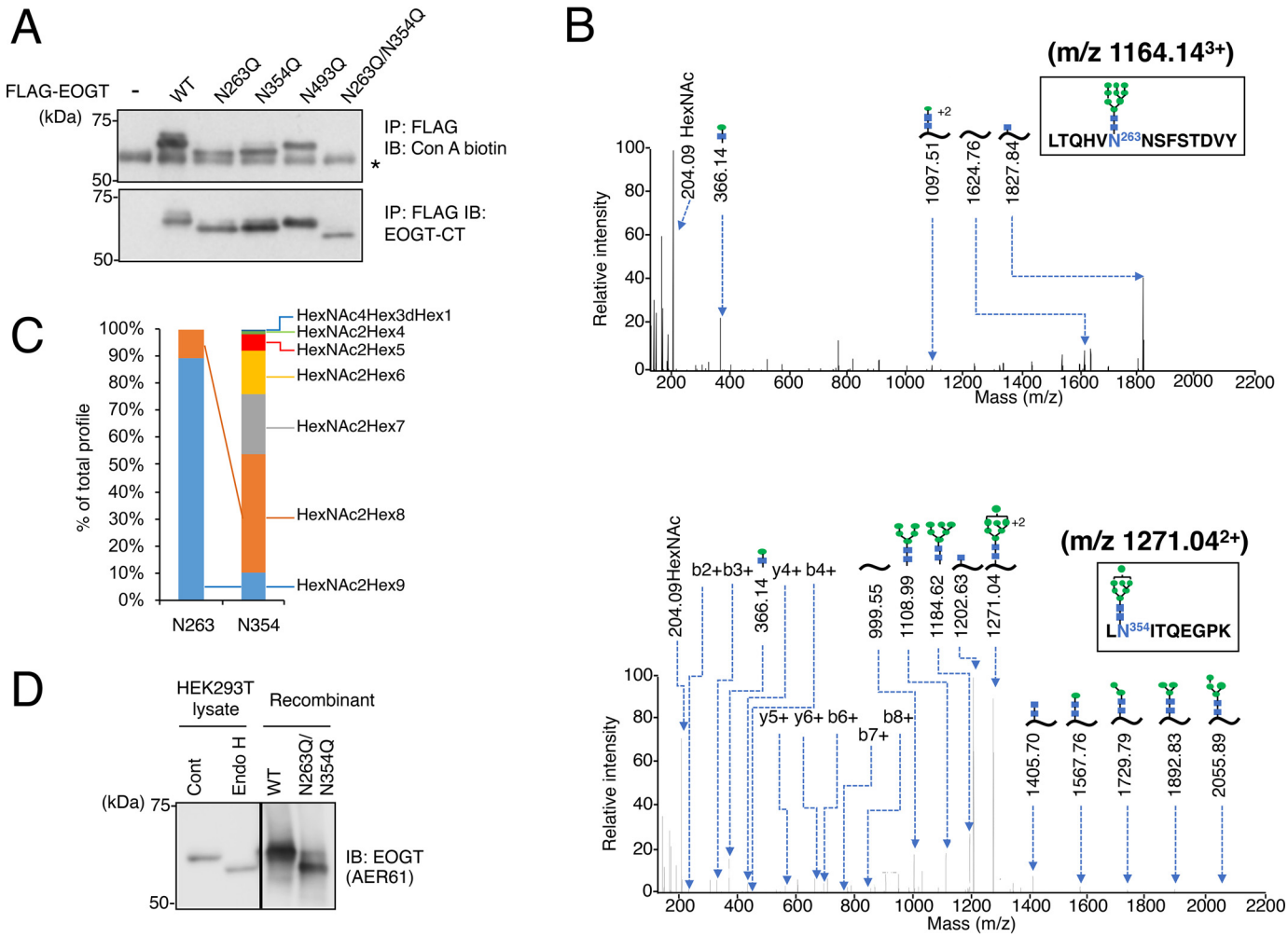

Figure 3. EOGT is modified with oligomannose *N*-glycans. *A*, lectin blot analysis of FLAG-EOGT isoforms. HEK293T cells were transfected to express each FLAG-EOGT isoform. The cell lysates were subjected to immunoprecipitation with FLAG-antibody followed by detection by biotinylated ConA lectin (*ConA-biotin*) or EOGT-CT antibody. An *asterisk* indicates nonspecific bands. *B*, LC–MS/MS spectra of glycopeptides modified with HexNAc2Hex9 *N*-glycan at N263 (*top*) and HexNAc2Hex7 N-glycan at Asn-354 (*bottom*) of FLAG-EOGT. Chymotryptic or tryptic glycopeptides prepared from recombinant FLAG-EOGT were analyzed by LC–MS/MS. Fragments ions corresponding to *b* and *y* ions, peptides with truncated glycans, and glycans are shown by *arrows*. *Blue square*, HexNAc (presumably GlcNAc); *green circle*, hexose (presumably mannose). *C*, bar graphs showing relative abundance of different *N*-glycan glycoforms at EOGT Asn-263 and Asn-354. *D*, endogenous EOGT sensitivity to Endo H digestion. HEK293T cell lysates were incubated in the absence or presence of Endo H and analyzed by immunoblotting with EOGT-specific AER61 antibody. Recombinant FLAG-EOGT and FLAG-EOGT$^{N263Q/N354Q}$ were analyzed in parallel as controls.

efficient cis-Golgi retrieval of KDEL-containing proteins (Fig. S2).

To confirm the oligomannose *N*-glycans on endogenous EOGT, HEK293T cell lysates were digested by endoglycosidase H (Endo H), which cleaves oligomannose-type and some hybrid-type, but not complex *N*-glycans. Endogenous EOGT, upon Endo H digestion, exhibited mobility shift compared with untreated EOGT and co-migrated with the *N*-glycan–deficient N263Q/N354Q FLAG-EOGT mutant (Fig. 3*D*). These results support the idea that endogenous EOGT is similarly modified with oligomannose *N*-glycans.

Removal of N-glycans from EOGT affects O-GlcNAcylation of Notch1

To determine whether *N*-glycans on Eogt are required for *O*-GlcNAcylation in cultured cells, endogenous *EOGT* genes in HEK293T cells were removed by CRISPR/Cas9-mediated gene editing and replaced with exogenously introduced FLAG-EOGT isoforms. All *EOGT* alleles in a population of cells derived from a single cell contain frameshift mutations and are considered as null (Fig. 4*A*). EOGT antibodies used in our previous study and the EOGT-CT antibody failed to detect EOGT at the endogenous level. In contrast, the most recent commercially available antibody (AER61 antibody) raised against the amino-terminal EOGT was highly sensitive for the detection of endogenous EOGT in the WT cells. Moreover, immunoblotting with the AER61 antibody exhibited no irrelevant bands, suggesting that it is highly specific to EOGT (Fig. 4*B*). These results also confirmed that *EOGT*-deficient HEK293T cells lack EOGT expression at the protein level.

Exogenous FLAG-EOGT was co-expressed with a membrane-tethered Notch1 fragment containing EGF repeats (*i.e.* FLAG-Notch1-TM) that serve as a reporter substrate to monitor *O*-GlcNAc levels. FLAG-Notch1-TM was affinity purified from the cell lysates of *EOGT*-deficient HEK293T cells, and the

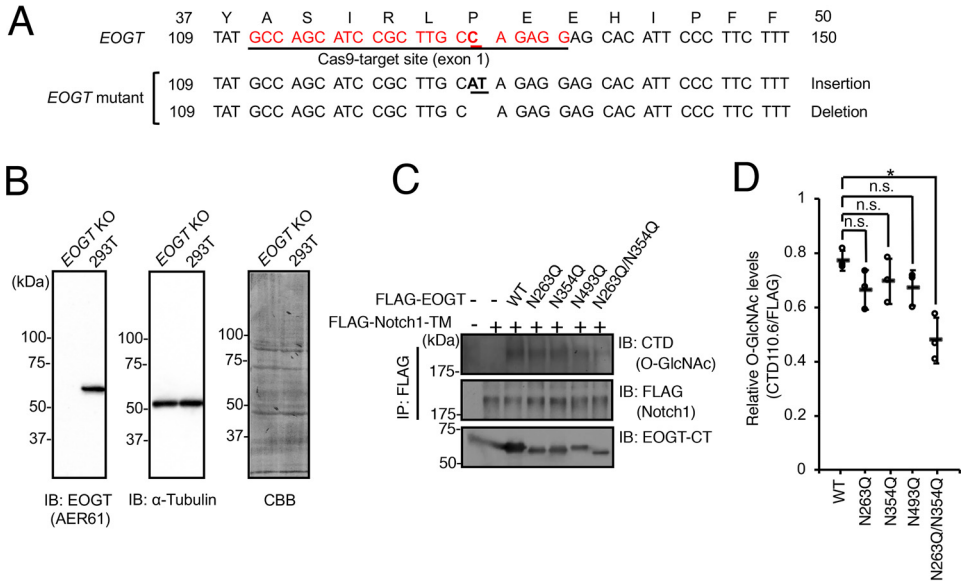

Figure 4. *N*-Glycans on EOGT are required for efficient *O*-GlcNAcylation. *A*, schematic representation of mutant alleles for *EOGT* newly generated by CRISPR/Cas9-mediated gene editing in HEK293T cells. *B*, detection of endogenous EOGT in cell lysates of HEK293T cells or *EOGT*-knockout (*KO*) HEK293T cells using EOGT-specific AER61 antibody. The immunoblot (*IB*) was re-probed using an α-tubulin antibody and stained with Coomassie Briliant Blue (*CBB*) as the protein loading control. *C*, immunoblotting with CTD110.6 antibody for detection of *O*-GlcNAc epitopes on FLAG-Notch1-TM. *EOGT*-knockout HEK293T cells were transfected to express FLAG-Notch1-TM together with WT or mutant *Eogt*. After purification with FLAG antibody-coated beads, FLAG-Notch1-TM was analyzed using the indicated antibodies. *D*, quantification of the relative *O*-GlcNAc level on FLAG-Notch1-TM. The band intensity, as shown in *C*, was measured using ImageJ software. The data were obtained from three independent transfection experiments and presented together with mean ± S.D. values. *, $p < 0.01$; the *p* values are from unpaired Welch's *t* test.

O-GlcNAc level was measured by immunoblotting with the CTD110.6 antibody. The antibody reactivity was not affected by the removal of a single *N*-glycosylation site, whereas simultaneous mutations (N263Q/N354Q) resulted in a significant decrease in the CTD110.6 reactivity (Fig. 4, *C* and *D*). These results indicate that a single *N*-glycan on EOGT is sufficient for *O*-GlcNAcylation.

Reduced O-GlcNAc stoichiometry in HEK293T cells expressing N-glycan–deficient EOGT

Although diminished CTD110.6 reactivity indicates a decreased *O*-GlcNAc level, there are caveats to this interpretation, because any elongation of the *O*-GlcNAc glycan precludes detection with the CTD110.6 antibody. Moreover, the CTD110.6 antibody could cross-react with other GlcNAc-containing glycan epitopes (3, 12, 13). To precisely investigate the decreased *O*-GlcNAc stoichiometry on Notch1 by loss of *N*-glycans, purified FLAG-Notch1-TM was subjected to MS (Fig. 5, *A* and *B*). Our previous studies revealed that several EGF domains on secreted Notch1 EGF repeats exhibit extended *O*-GlcNAc structures including O-GlcNAc-Gal or *O*-GlcNAc-Gal-Sia (14). Unexpectedly, elongated *O*-GlcNAc glycans were undetectable on the transmembrane form of Notch1. This is likely because transiently expressed membrane-tethered Notch1 is not efficiently transported to the cell surface but rather retained in the ER as an *O*-GlcNAc monosaccharide form. Nonetheless, we were able to compare the *O*-GlcNAc stoichiometry of various EGF domains catalyzed by WT EOGT *versus* the N263Q/N354Q mutant. The semi-quantitative analysis revealed that *O*-GlcNAc stoichiometry is significantly decreased in EGF10, EGF21, and EGF23 in the absence of *N*-glycans (Fig. 5 and Fig. S3). Other EGF domains including EGF2 and EGF10 similarly showed decreased *O*-GlcNAc stoichiometry, although they are not statistically significant in duplicate samples. In contrast, *O*-fucose and *O*-glucose modifications are comparable between WT and the N263Q/N354Q FLAG-EOGT (Fig. S4). Taken together, these data suggested that *N*-glycans on EOGT impact its ability to *O*-GlcNAcylate a wide range of EGF domains, rather than specific domains of Notch1.

N-glycans are dispensable for the enzymatic activity of EOGT

To determine whether enzyme activity is affected by the loss of *N*-glycans, an *in vitro* EOGT assay was performed using *Drosophila* Notch EGF20 (dEGF20) as a model substrate (1). The His-tagged dEGF20 was bacterially expressed and purified by immobilized metal ion affinity chromatography and HPLC (Fig. 6*A*). The correct folding of the purified dEGF20 domain was confirmed by its ability to serve as a substrate for POFUT1, POGLUT1, and EOGT (15, 16) (Fig. 6*B* and data not shown). For the evaluation of the *O*-GlcNAc transferase activity of mutant EOGT, UDP-Glo assay was performed using dEGF20 as an acceptor substrate, UDP-GlcNAc as a donor substrate, and purified EOGT constructs (Fig. 6*C*). No significant differences in enzyme activity were detected in each mutant compared with WT EOGT. The activity of the N263Q/N354Q mutant was also confirmed using HPLC (Fig. 6*D*). These data suggest that *N*-glycans are dispensable for the *O*-GlcNAc transferase activity of EOGT.

N-Glycans facilitate the maturation of EOGT

To address the effect of *N*-glycans on EOGT expression levels, WT or mutant EOGT were co-expressed with GFP, which

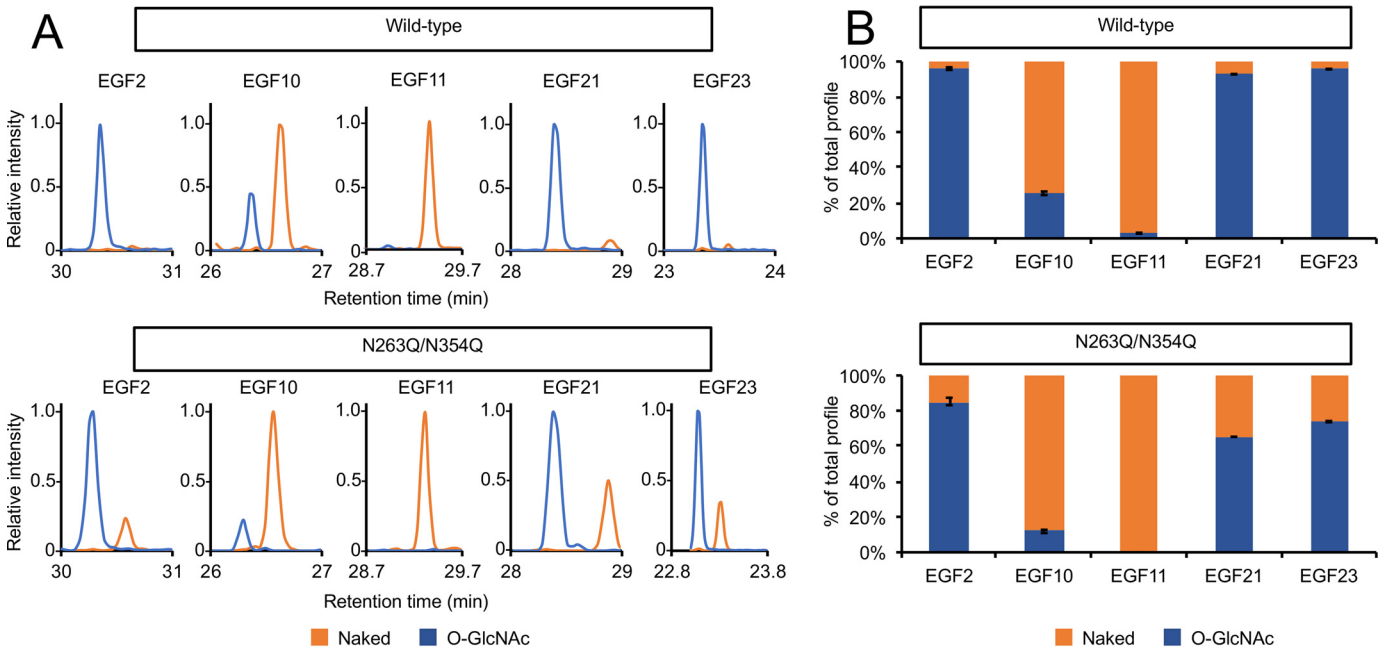

Figure 5. Reduced *O*-GlcNAc stoichiometry on Notch1 in HEK293T cells expressing *N*-glycan-deficient EOGT. *A*, MS analysis of tryptic glycopeptides prepared from FLAG-Notch1-TM harboring *O*-GlcNAcylation sites. FLAG-Notch1-TM was expressed in *EOGT*-deficient HEK293T cells exogenously expressing WT or the N263Q/N354Q EOGT. EICs show the relative signal intensity corresponding to the peptides without modification (*orange*) or with *O*-GlcNAc (*blue*) on EGF2, EGF10, EGF11, EGF21, and EGF23 of Notch1. Note that no elongated *O*-GlcNAc glycoforms were detected. Data are presented as mean ± S.D. ($n = 2$). LC–MS/MS spectra of tryptic glycopeptides are shown in Fig. S3. *B*, quantification of *O*-GlcNAc glycans on representative EGF domains. EIC peak heights were measured and expressed as percent area. The color code is same as described in *A*.

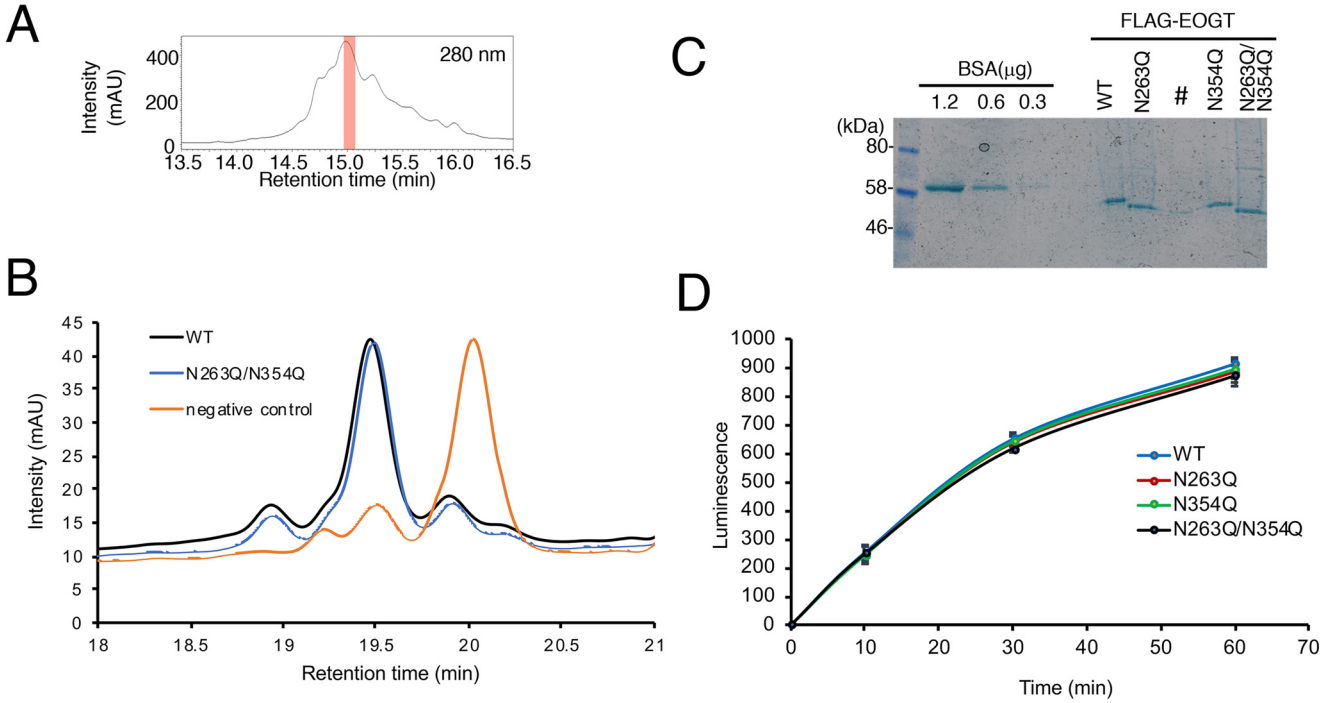

Figure 6. *N*-Glycans are dispensable for the enzymatic activity of EOGT. *A*, bacterially expressed dEGF20 was analyzed by HPLC with a 30-min linear gradient (10–80% ACN in 0.1% TFA). Absorbance at 280 nm was monitored. The fraction containing folded dEGF20 is highlighted in *red*. *B*, HPLC analysis of enzymatic products. *In vitro O*-GlcNAc transferase assay was performed using dEGF20 as an acceptor substrate, UDP-GlcNAc as a donor substrate, and WT or mutated FLAG-EOGT as an enzyme or buffer as a negative control. *C*, Coomassie staining showing the purified WT and mutant FLAG- EOGT. An empty well is marked by #. *D*, the enzymatic activities of the respective FLAG-EOGT isoforms measured by UDP-Glo assay using an equal amount of purified enzymes. The results are expressed as mean ± S.D. from three assays performed independently.

was linked to the *Eogt* transgene via an internal ribosome entry site (IRES) sequence (Fig. 7*A*). Quantification of the EOGT level normalized to GFP revealed that the N263Q/N354Q mutant expression was decreased by 66% compared with WT EOGT (Fig. 7*B*). In contrast, the difference between the expression levels of the WT and single-site mutant EOGT proteins

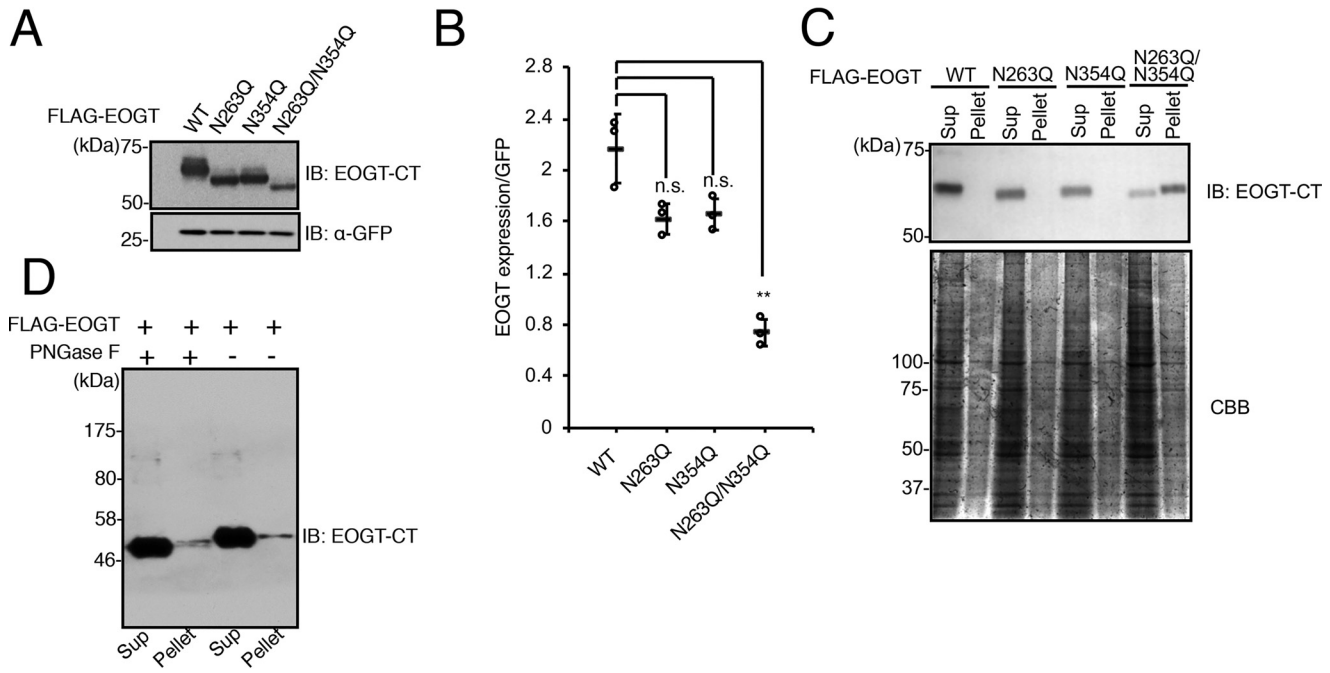

Figure 7. *N*-Glycans affect the protein expression of EOGT. *A*, immunoblot (*IB*) analysis for protein expression of WT and mutant EOGT. Each FLAG-EOGT isoform was co-expressed together with GFP that served as an internal control of protein expression in HEK293T cells. Cell lysates were analyzed with an EOGT-CT or a GFP antibody. *B*, quantification of EOGT protein levels normalized to GFP. The data were obtained from three independent transfection experiments and presented together with mean ± S.D. values. **, $p < 0.05$; the *p* values are from unpaired Welch's *t* test. *C*, detection of FLAG-EOGT isoforms in the soluble and insoluble fractions. Cells stably expressing WT or mutant EOGT were lysed in TBS buffer containing 0.1% digitonin. Soluble/insoluble fractions were separated and detected with an EOGT-CT antibody. After immunoblotting, the PVDF membrane was stained with Coomassie Brilliant Blue (*CBB*) as the protein loading control. The data are representative of two independent transfection experiments. *D*, purified FLAG-EOGT was incubated with or without PNGase F. After 3 h, soluble/insoluble fractions of reaction mixtures were separated and detected with EOGT-CT antibody. *n.s.*, not significant.

was statistically insignificant. Tunicamycin treatment reduced the expression of WT and N263Q or N354Q single mutants, but not the N263Q/N354Q double mutant (Fig. 2*C*). These effects are consistent with the presence or absence of *N*-glycans on each EOGT isoform. Taken together, these results suggested that *N*-glycans affect the expression level of EOGT.

As a molecular basis for the decreased expression of the N263Q/N354Q protein, *N*-glycan could affect the protein folding or stability and thus protein expression of EOGT. To test this idea, we separated and characterized the soluble and insoluble fractions of cell lysates prepared from HEK293T cells stably expressing each EOGT isoform. In the presence of mild detergents (0.1% digitonin), WT EOGT was found in the soluble fractions. Although the loss of single *N*-glycan lead to no obvious solubility changes, the N263Q/N354Q mutant showed increased insolubility compared with WT EOGT (Fig. 7*C*). These results indicated that *N*-glycans facilitated the expression of the matured form of EOGT, and thus maintained the protein expression required for normal protein function.

To test the idea that *N*-glycans directly affect EOGT solubility or stability, *N*-glycans were removed from WT EOGT *in vitro* using PNGase F (Fig. 7*D*) and Endo H (data not shown). Fractionation into soluble and insoluble fractions revealed that the loss of *N*-glycans did not change the amount of the soluble EOGT form. Moreover, the purified N263Q/N354Q EOGT mutant remains soluble at the concentration of 0.04 mg/ml (data not shown). These data suggest that *N*-glycans do not affect EOGT stability or solubility, but facilitate the generation of a matured EOGT form, possibly through the promotion of protein folding.

N-glycans on EOGT are required for its peripheral ER localization

Although *N*-glycans are important for subcellular localization of Golgi glycosyltransferases, their effect on ER glycosyltransferases has not been previously addressed. The ER is composed of distinct domains, including the ribosome-studded perinuclear ER sheets and peripheral smooth peripheral tubules (17, 18). As previously described, the ER-resident chaperone calnexin was distributed in both the peripheral and perinuclear ER (Fig. 8*A*) (17).

To analyze the effect of *N*-glycans on the ER localization of EOGT, the alteration in the subcellular localization of each EOGT mutant was analyzed. As previously reported, WT EOGT was detected throughout the ER in HEK293T cells. The single mutants (N263Q or N354Q) exhibited a similar staining intensity and pattern with WT EOGT. In contrast, the staining intensity of the double mutant (N263Q/N354Q) was apparently weaker than the WT. Although we could readily observe the perinuclear EOGT staining, the signal at the ER periphery visibly decreased (Fig. 8, *A* and *B*). Quantification of peripheral to perinuclear staining ratio confirmed that EOGT distribution to the peripheral region is significantly decreased when *N*-glycans are removed from EOGT. Of note, a soluble form of Notch1 EGF repeats can distribute to the peripheral ER irrespective of co-expression of WT or the N263Q/N354Q mutant EOGT (Fig. 8, *C* and *D*). These results suggest that *N*-glycans affect the peripheral distribution of EOGT in the ER.

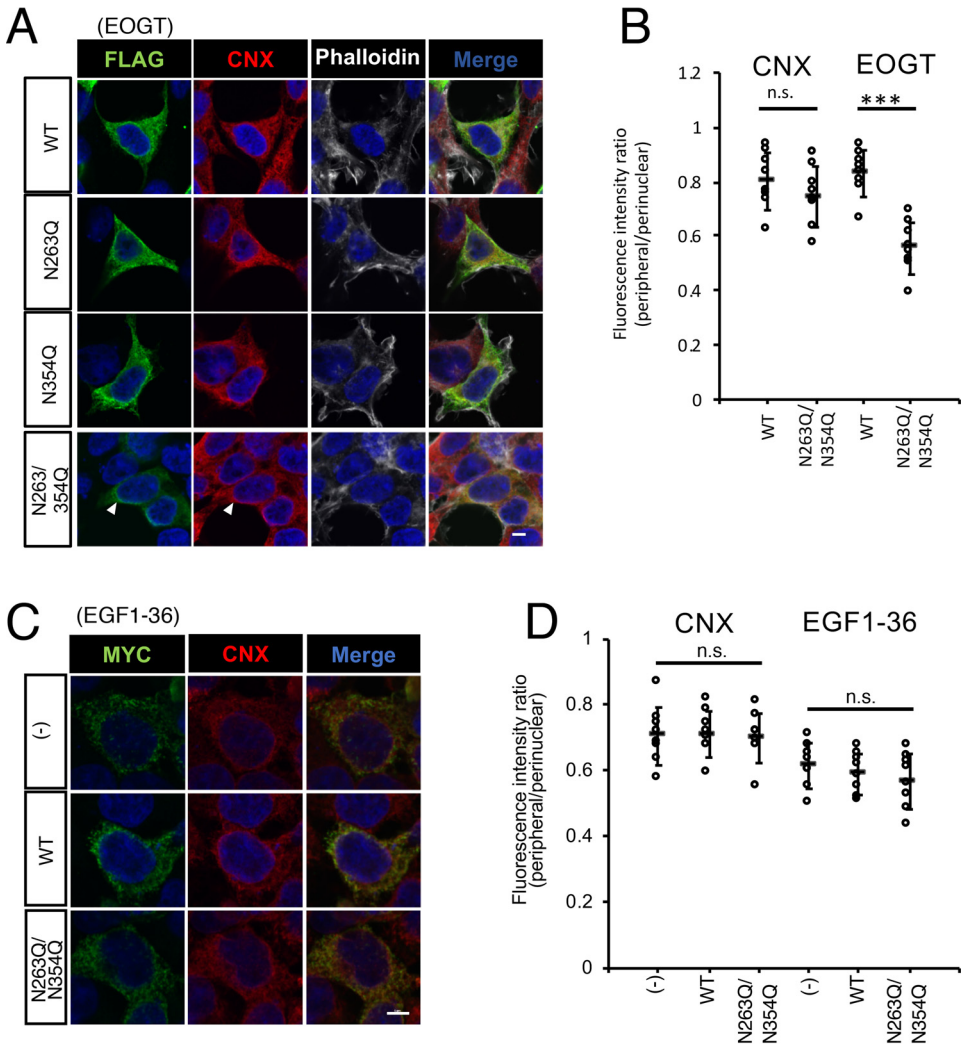

Figure 8. Loss of *N*-glycans on EOGT diminished its peripheral ER localization. *A*, subcellular localization of FLAG-EOGT and EOGT mutants. Confocal microscopy was performed on HEK293T cells transiently transfected with WT *FLAG-Eogt* or one of its *N*-glycosylation mutants. Staining was performed with anti-FLAG (for EOGT, *green*), anti-calnexin (ER marker, *red*), and phalloidin (*white*). It is noted that EOGT staining at cell periphery is diminished, whereas the perinuclear staining remained in the N263Q/N354Q mutant (*arrowheads*). *Scale bar*, 5 μm. Additional data are shown in Fig. S5*A*. *B*, staining intensity ratio between peripheral and perinuclear regions in the images shown in *A*. The results were obtained from eight transfected cells in a single experiment. Similar results were obtained in three independent transfection experiments. Data are presented as mean ± S.D. ***, $p < 0.001$; the *p* values are from unpaired Welch's *t* test. *C*, subcellular localization of Notch1EGF1-36:MycHis. Confocal microscopy imaging was performed on HEK293T cells transiently transfected with *Notch1EGF1-36:MycHis* alone or together with *FLAG-Eogt* or its mutant. Staining was performed with anti-Myc (for Notch1EGF1-36, *green*) and anti-calnexin. *Scale bar*, 5 μm. *D*, staining intensity ratio between peripheral and perinuclear regions in the images shown in *C*. The results were obtained from eight transfected cells in a single experiment. Similar results were obtained in three independent transfection experiments. Data are presented as mean ± S.D.

Effect of tunicamycin on the ER localization of endogenous EOGT

To study the effect of *N*-glycan loss on endogenous EOGT, we immunostained HEK293T cells using the EOGT-specific AER61 antibody. Endogenous EOGT showed a punctate staining pattern that was largely included in the calnexin-positive area. Indeed, no staining was detected in negative control cells lacking *EOGT* expression (Fig. 9*A*).

To analyze the effect of *N*-glycans on the distribution of endogenous EOGT, HEK293T cells were treated with tunicamycin. As expected, upon tunicamycin treatment, the EOGT staining markedly decreased, which was most evident at the cell periphery. Consistently, the ratio of EOGT staining at the peripheral ER *versus* perinuclear ER was significantly decreased. In contrast, calnexin distribution within the ER was comparable between tunicamycin-treated *versus* untreated cells (Fig. 9, *B* and *C*). To exclude the possibility that tunicamycin-induced ER stress could contribute to the observed changes in EOGT subcellular localization, HEK293T cells were treated with thapsigargin that depletes the Ca^{2+} stored in the ER and causes ER stress. Unlike tunicamycin, thapsigargin had little impact on the EOGT distribution. Taken together, these results indicate that *N*-glycans on EOGT facilitate its distribution at the periphery of the ER.

To further explore the effect of *N*-glycans on EOGT in other cultured cells, HeLa cells were treated with tunicamycin or thapsigargin. Similar to HEK293T cells, tunicamycin treatment resulted in decreased EOGT staining at the peripheral ER (Fig. 9, *B* and *C*). Since EOGT regulates Notch signaling in endothelial cells, we further analyzed the effect of tunicamycin on

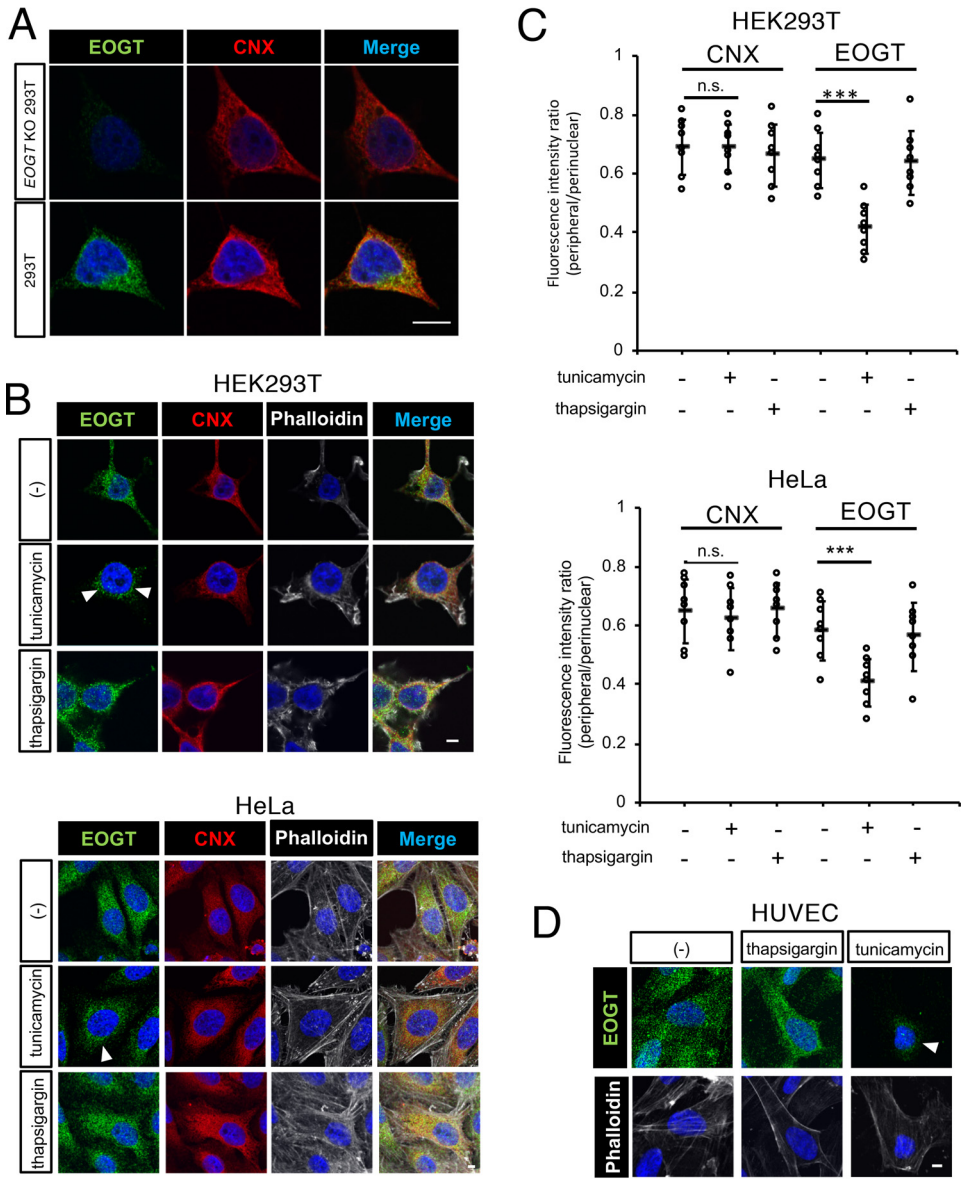

Figure 9. Decreased peripheral ER localization of endogenous EOGT in cells treated with tunicamycin. *A*, detection of endogenous EOGT by the specific AER61 antibody. *B*, subcellular localization of endogenous EOGT in HEK293T or HeLa cells. Cells were treated with or without tunicamycin for 48 h and stained with the EOGT-specific AER61 (*green*) antibody, calnexin (*red*) antibody, and phalloidin (*white*). *Scale bar*, 5 μm. *C*, staining intensity ratio between peripheral and perinuclear regions in the images shown in *B*. The results were obtained from eight transfected cells in a single experiment. Similar results were obtained in three independent transfection experiments. Data are presented as mean ± S.D. ***, $p < 0.001$; the *p* values are from unpaired Welch's *t* test. *D*, subcellular localization of endogenous EOGT in endothelial cells. HUVEC cells were treated with or without tunicamycin for 48 h and stained with the EOGT-specific AER61 (*green*) antibody and phalloidin (*white*). *Scale bar*, 5 μm.

human umbilical vein endothelial cells (HUVEC). Although the overall EOGT staining intensity decreased upon tunicamycin treatment, the peripheral ER staining diminished prominently in HUVEC cells (Fig. 9*D*). Taken together, these results demonstrate that *N*-glycans are generally required for the peripheral EOGT distribution.

Discussion

N-Glycans are present on various glycoproteins and affect their folding, stability, trafficking to the cell surface, and molecular function (19); thus, they are essential for developmental processes (20). *N*-Glycosylation is initiated at the ribosome-translocon complex that includes STT3 as a catalytic subunit of oligosaccharyltransferases (21). Recently, the STT3 inhibitor NGI-1 was developed and shown to inhibit the growth of non-small-cell lung cancer cells by suppressing the cell-surface expression and signaling of the epidermal growth factor receptor (22). Thus, the inhibition of a synthetic pathway for *N*-glycosylation holds a promise to represent a novel approach in cancer treatment (23–26).

In this study, we have performed in-depth analysis of the *N*-glycan structure and function on the ER luminal *O*-GlcNAc transferase EOGT. Among the three putative *N*-glycosylation sites (Asn-263, Asn-354, and Asn-493) in mouse EOGT, we determined that only Asn-263 and Asn-354, but not Asn-493, are modified with oligomannose *N*-glycans. The lack of

modification at N493Y/N493S could be explained based on the fact that C-terminal sequons within the last 50 amino acids are modified post-translationally by STT3B isoform of the OST that prefer NXT sites over NXS sites (27).

In mammals, both Asn-263 and Asn-354 sites are highly conserved except for *O. cuniculus* (rabbit), in which N354I/N354T is changed to N354I/N354A. Rabbit EOGT does not contain additional potential *N*-glycan sites, suggesting that only single *N*-glycan is sufficient for EOGT function. Consistent with this view, our results showed that neither N263Q nor N354Q mutation affects the ability of mouse EOGT to *O*-GlcNAcylate Notch1. In humans, somatic mutations corresponding to the *N*-glycosylation sequons are observed in the ICGC cancer database, and some of them are classified as potentially pathogenic (Fig. 1*A*). However, our results suggest that these mutations are pathogenic, only if two types of mutations occur coincidently and result in the simultaneous loss of both *N*-glycans.

Given that *N*-glycans are prevalent modifications, virtually all glycosyltransferases are modified or predicted to be modified with *N*-glycans with the exception of intracellular *O*-GlcNAc transferase OGT (28). Compelling experimental evidence regarding Golgi glycosyltransferase suggests that *N*-glycans are required for enzyme activity (29–33) and/or Golgi localization (31, 32, 34). Analysis of GM3 synthase further demonstrated that *N*-glycans affect the protein stability of the glycosyltransferase (34). In contrast, only a few studies are addressing the roles of *N*-glycans in ER glycosyltransferase. In addition to the function of POFUT1 *N*-glycans in protein solubility and enzyme activity, *N*-glycans on POMT1 or POMT2 are required for enzyme activity (35). In line with these observations, our study showed the critical roles of *N*-glycans in EOGT function in the ER.

N-Glycans are bulky amphipathic modifications that promote protein folding and stabilize proteins in native states via carbohydrate-protein interactions (36). In the current study, the complete removal of *N*-glycans on EOGT resulted in a decrease of the soluble EOGT form in cultured cells. The effect of *N*-glycans on sustaining protein expression is consistent with established roles of *N*-glycans on protein stability and folding during protein maturation. In contrast, *N*-glycan deficiency did not impair *in vitro O*-GlcNAc transferase activity. These observations indicate that *N*-glycans facilitate the generation of matured EOGT protein, but not its enzyme activity.

The ER is a membrane-delineated organelle consisting of central ER sheets decorated with membrane-bound ribosomes and peripheral ER. Recently, super-resolution microscopy revealed that the peripheral ER represents tight or loose arrays of tubular network (18). Various endogenous ER proteins localize in the peripheral ER tubules, including calnexin, Derlin-1, Bip/GRP78, glycoprotein 78/Gp78, and syntaxin 17 (17, 37). Furthermore, single-molecule super-resolution particle tracking indicated the existence of an active ER luminal flow in peripheral ER tubules (38). In our study, EOGT localized at both the perinuclear and peripheral ER as with calnexin. Importantly, the *N*-glycan–deficient FLAG-EOGT mutant was localized predominantly in the perinuclear ER due to the loss of staining in the peripheral ER. Similarly, tunicamycin treatment suppressed the peripheral ER localization of endogenous EOGT. Therefore, *N*-glycans *per se* or *N*-glycan–dependent structural aspects on EOGT may facilitate its diffusion from the perinuclear to peripheral ER. To the best of our knowledge, this is the first study to show that *N*-glycans mediate the correct distribution of ER-resident proteins within the ER. Although the overall EOGT expression level decreased in the absence of *N*-glycans, EOGT immunostaining nearly diminished in the peripheral ER, whereas perinuclear EOGT staining was still detectable. Thus, the decreased *O*-GlcNAc stoichiometry on Notch1, mediated by the absence of *N*-glycans on EOGT, could not only be attributed to the overall EOGT protein expression level but also the altered subcellular EOGT localization in the ER.

Multidomain proteins such as the Notch receptors could be folded co-translationally and post-translationally (39). Since EOGT acts specifically on the folded EGF domain, an *O*-GlcNAc modification may occur during translation and after the partially folded intermediates are released from the ribosome. Since the peripheral ER is largely devoid of ribosomes, if peripheral EOGT has a role in Notch glycosylation, it would act on the partially folded intermediate of Notch EGF repeats. Several chaperones including calnexin and Bip/GRP78 were shown to localize in the peripheral ER (17). Together with other chaperones, EOGT may be involved in the protein maturation process in the peripheral ER, wherein newly formed EGF domains are sequentially *O*-GlcNAcylated to complete their *O*-glycosylation along with correct folding of the entire EGF repeats. Future studies should determine whether *O*-GlcNAcylation occurs in the peripheral ER. Moreover, comprehensive and comparative analysis of other ER-localized glycosyltransferases such as POFUT1, POGLUT1, POGLUT 2, and POGLUT 3 (40) should be performed to get insight into the presence of distinct ER domains specialized in the maturation of Notch receptors and other EGF domain-containing proteins.

Experimental procedures

Sequence alignment

The amino acid sequences of EOGT from different species were collected from the NCBI protein database. Accession numbers of the protein sequences are: *M. musculus* NP_780522.1, *R. norvegicus* NP_001009502.1, *O. cuniculus* XP_002713346.1, *B. taurus* NP_001071350.1, *S. scrofa* NP_001302603.1, *H. sapiens* NP_001265618.1, and *C. lupus familiaris* NP_001009187. The amino acid sequence homology of EOGT was performed using the Clustal Omega program by the European Bioinformatics Institute (EMBL-EBI) available at RRID:SCR_001591.

Antibody information

The antibodies used are described in Table S1. We generated a rabbit anti-EOGT-CT antibody using the HVLQHPKWPFKKKHDEL peptide as an antigen.

Plasmid constructs

pSectag2C/*mNotch1EGF1-36:MycHis-IRES-EGFP* was a generous gift from Dr. Pamela Stanley (41). pSectag2C/*Eogt-IRES-GFP* has been described previously (2). To generate

pET22b(+)/*dEGF20His*, dEGF20 fragments of pMT-Bip/*dEGF20:V5His* (1) were excised using XhoI and BamHI and inserted into the same sites of pET22b(+) (Novagen). Site-directed mutagenesis for the generation of *N*-glycosylation site mutants was performed using the PrimeSTAR mutagenesis kit (Takara Bio) with pSectag2C/*Eogt-IRES-EGFP* as a template DNA. To generate the FLAG-EOGT expression vector, a FLAG tag was inserted into *Eogt* cDNA after the codon at Lys-32 of pSectag2C/*Eogt-IRES-EGFP* utilizing the PrimeSTAR mutagenesis kit (Takara Bio). The tag remains on EOGT after the liberation of its signal peptide. To generate mutant forms of FLAG-EOGT vectors, the AflII/ApaI fragment of WT FLAG-EOGT was replaced with those corresponding to the mutant FLAG-EOGT. The successful construction of the vectors was confirmed by DNA sequencing.

For the generation of an expression vector for the FLAG-tagged Notch1 transmembrane construct (*FLAG-Notch1-TM*), the EcoRI/AfeI fragment of synthetic oligonucleotides containing the Igκ signal sequences and FLAG tag sequences was ligated with an AfeI/XbaI fragment of mouse *Notch1-TM* spanning from EGF1 to LIN-12/Notch Repeat 3 (LNR3) (nucleotide numbers 55-5738: amino acid sequence 19-1916), and cloned into pTracer-CMV vector. Primers and the synthetic oligonucleotides used in this study are shown in Table S2.

Cell culture and transfection

Cells were cultured in Dulbecco's modified Eagle's medium (DMEM) supplemented with 7.5% heat-inactivated fetal bovine serum (FBS) and 1% penicillin-streptomycin at 37 ℃ and 5% CO_2. Expression vectors were transiently transfected using polyethyleneimine (PEI, MW 40,000, Polysciences) and insulin-transferrin-selenium (ITS)/DMEM without FBS and antibiotics as described previously (4). Briefly, 1 μg of plasmid DNA was added to 200 μl of ITS/DMEM and mixed with 5 μg of PEI followed by 20 min incubation at room temperature. Then, the DNA/PEI mixture was added to the cells of 6-well–plates pretreated with 800 μl of ITS/DMEM. After 6-12 h of incubation at 37 ℃ with 5% CO_2, the medium was changed with 2 ml of 10% FBS/DMEM containing 1% penicillin/streptomycin. Cells were incubated for another 48 h before the analysis.

EOGT-knockout HEK293T cells were newly generated using CRISPR/Cas9-mediated gene targeting as described previously (4). In brief, a plasmid expressing GFP-Cas9 in addition to guide RNA, which encodes a single guide RNA that targets the first exon of human *EOGT*, was used to transfect HEK293T cells. Single cells successfully expressing Cas9-GFP were collected. The removal of the targeted gene region was confirmed by sequencing analysis.

Generation of stable cell lines

HEK293T cells were transfected with pSectag2C/*FLAG-Eogt-IRES-EGFP* or one of the EOGT mutants. After 24 h, cells were diluted 10 times, and their culture with 100 μg/ml of hygromycin B in 10% FBS/DMEM with 1% penicillin-streptomycin was initiated. Medium was changed every 3 days with hygromycin until colonies were formed. The single colony was transferred into 96-well culture plates. Surviving cells were expanded and maintained in the presence of hygromycin B.

EOGT deglycosylation

PNGase F treatment was carried out according to the manufacturer's protocol (New England Biolabs). In brief, WT or mutant FLAG-EOGT was immunoprecipitated from lysates of transfected HEK293T cells using anti-FLAG antibody-conjugated magnetic beads (M185-10, MBL). Then, an *N*-glycanase reaction was performed at nondenatured conditions using 0.5 μl of PNGase F (1 unit/μl, Roche) in G7 reaction buffer (New England Biolabs) at 37 ℃. Endo H digestion was performed by treating cell lysates with 1 μl of Endo H (New England Biolabs) in 30 mM sodium acetate (pH 6.0) at 37 ℃ for 1 h. The samples were separated by 7.5% SDS-PAGE followed by immunoblotting with rabbit anti-EOGT-CT antibody as described below.

Immunoblotting

Cells were lysed in lysis buffer containing Tris-buffered saline, pH 7.6 (TBS), 1 mM $CaCl_2$, and 1% Nonidet P-40. The lysate was denatured using SDS-PAGE sample buffer. For Western blotting, each sample was separated by 7.5% SDS-PAGE and transferred onto a PVDF membrane (Millipore). The membrane was blocked in blocking buffer (3% skim milk and 0.05% polysorbate 20 in PBS) at room temperature for 30 min followed by incubation with the appropriate primary antibody diluted in blocking buffer at room temperature for 1 h. After washing with 0.05% polysorbate 20 in PBS (PBS-T) three times, the membrane was incubated with horseradish peroxidase (HRP)-conjugated secondary antibody in blocking buffer at room temperature for 1 h. After the membrane was washed with PBS-T three times for 10 min, the desired band on the membrane was visualized with Immobilon Western Chemiluminescent HRP Substrate (Millipore) and afterward being exposed to X-ray film (Fujifilm).

Tunicamycin and thapsigargin treatments

Immediately after transfection, the cells were grown in the presence or absence of 2 μg/ml of tunicamycin (Sigma) for 48 h. Then, cell lysates were prepared and analyzed by immunoblotting using anti-FLAG or rabbit anti-EOGT-CT, anti-GFP antibody, or anti-α-tubulin antibody. For immunostaining, HEK293T cells were cultured with or without 2 μg/ml of tunicamycin for 48 h. *EOGT*-deficient HEK293T cells were used as a negative control. Rabbit anti-EOGT (AER61) and mouse anti-calnexin antibodies were used to detect endogenous EOGT and calnexin (as an ER marker), respectively.

For the experiments with thapsigargin, HEK293T cells were grown with or without 5 μM thapsigargin (Wako) for 48 h. The immunostaining was performed as described above.

Lectin blotting

Anti-FLAG antibody-conjugated magnetic-agarose beads (MBL) were used to purify WT or mutant FLAG-EOGT from the cell lysates of transfected HEK293T cells. Then, the proteins were separated by SDS-PAGE and transferred onto a

PVDF membrane followed by blocking with blocking buffer containing 3% BSA (BSA) in PBS-T at room temperature for 30 min. Next, the membrane was incubated with ConA-biotin (MBL) diluted in blocking buffer (1:1000 dilution) at room temperature for 1 h. After washing with PBS-T three times, the membrane was incubated with avidin-HRP (1:1000 dilution in blocking buffer) at room temperature for 1 h. After the membrane was washed with PBS-T for 10 min three times, the bands on the membrane were visualized with Immobilon Western Chemiluminescent HRP Substrate (Millipore) and X-ray films (Fujifilm).

Purification of EOGT

WT or mutant FLAG-EOGT was purified from the respective stable cell line. In brief, cells were lysed in lysis buffer as described above by incubation for 15 min on ice. Then, samples were centrifuged at 15,000 × *g* at 4 °C for 15 min. The supernatant was collected as cell lysate. The lysates were mixed with anti-FLAG antibody-conjugated magnetic beads and incubated at 4 °C overnight with gentle rotation. Next, the beads were washed extensively with the lysis buffer and eluted with 50 μl of 3× FLAG peptides (1 μg/μl, MBL) in 10 mM HEPES, pH 7.0. Unbound 3× FLAG peptides were removed by Amicon Ultra-0.5 3K centrifugal filter device (UFC500396, Millipore). Protein quantification was performed by Coomassie Blue staining using Coomassie Brilliant Blue G-250 dye and BSA as a protein concentration standard.

Statistical methodology

The statistical analyses were performed utilizing Welch's *t test* as detailed in Table S3.

LC–MS/MS analysis of N-linked glycopeptides

WT FLAG-EOGT was stably expressed in HEK293T cells, purified using anti-FLAG antibody-conjugated magnetic-agarose beads (MBL), and eluted in 2× SDS sample buffer. After separation by 7.5% SDS-PAGE, bands were developed by Coomassie Blue staining. The band was cut into pieces, and the gel pieces were transferred into low-binding tubes. Then, gel pieces containing the desired proteins were destained using 50% methanol (MeOH) in 20 mM NH_4HCO_3 at 4 °C overnight. Acetonitrile (ACN) was added into the tubes, and the samples were dried using a speed-vacuum system for 20 min Subsequently, the samples were reduced with 10 mM DTT, 100 mM NH_4HCO_3 for 30 min followed by alkylation with 50 mM iodoacetamide, 100 mM NH_4HCO_3 for 30 min. Then, 5% acetic acid in 50% MeOH was added to the samples and incubated at 4 °C overnight. ACN was added to the samples and speed-vacuumed for drying. In-gel digestion was performed in 25 mM NH_4HCO_3 at 37 °C by incubating with 20 ng/μl of trypsin gold (Promega) for 16 h or 10 ng/μl of chymotrypsin (Roche Applied Science) for 5 h. The digested peptide samples were desalted using Ziptip (C18, Millipore) and dissolved in 0.1% TFA (TFA), 80% ACN. The peptides were analyzed by LC–MS on a Q-Exactive mass spectrometer (ThermoFisher) coupled to an UltiMate3000 RSLCnano LC system (Dionex Co., Amsterdam, The Netherlands) using a nano HPLC capillary column, 150 mm × 75 μm inner diameter (Nikkyo Technos Co., Japan) via a nanoelectrospray ion source. Reversed-phase chromatography was performed with a linear gradient (0 min, 5% B; 45 min, 100% B) of solvent A (2% ACN with 0.1% formic acid) and solvent B (95% ACN with 0.1% formic acid) at an estimated flow rate of 300 nl/min. A precursor ion scan was carried out using a 400–1600 *m/z* prior to MS2 analysis. Isolation of precursors was performed within a window of 2.0 Th by quadrupole. Collision-induced dissociation at stepped collision energies of 33 ± 13 was employed as a fragmentation method. MS2 scan was obtained for the 20 most intense precursor ions with an absolute intensity threshold of 1,700. *N*-Glycosylation was analyzed by Byonic (version 3.5), Proteome Discoverer (version 2.3), and Xcalibur (version 4.3) softwares (ThermoFisher). EOGT sequence was searched using trypsin or chymotrypsin protease specificity (Lys/Arg or Trp/Tyr/Phe) with a possibility of 1 or 2 missed cleavages, respectively, and a precursor mass tolerance of 10 ppm and a fragment mass tolerance of 20 ppm. Carbamidomethylation was selected as fixed modification on Cys residues. Variable modifications selected are summarized in Table S4. All peptide sequences assigned are shown in Table S5.

LC–MS/MS analysis of O-GlcNAcylation on Notch1

FLAG-Notch1-TM was transiently expressed in *EOGT*-deficient HEK293T cells, purified using anti-FLAG antibody-conjugated magnetic agarose beads, and eluted with 2× SDS sample buffer followed by separation by SDS-PAGE. Then, the samples were digested and cleaned up by Ziptip as described above. The peptides were analyzed by LC–MS on an Orbitrap Fusion mass spectrometer (ThermoFisher) coupled to an UltiMate3000 RSLCnano LC system with a nano-HPLC capillary column via a nanoelectrospray ion source as described above. A precursor ion scan was carried out using a 400–1600 *m/z* prior to the MS2 analysis. Isolation of precursors was performed with a window of 0.8 Th by quadrupole. High-energy collisional dissociation at stepped collision energies of 33 ± 13 was employed as a fragmentation method and rapid scan MS analysis was performed in an ion trap mass analyzer. Only those precursors with a charge state of 2–6 with an absolute intensity threshold of 5000 were sampled for MS2. The dynamic exclusion duration was set to 10 s with a 10 ppm tolerance. The instrument was run at top speed mode with 3-s cycles. The relative amounts of glycopeptides were calculated based on their EIC peak heights. The raw data were searched for *O*-linked glycopeptides using the GlycoPAT software (version 1.0) (42). Notch1 sequence was searched using trypsin protease specificity (Lys/Arg) with a possibility of 1 missed cleavage, and a precursor mass tolerance of 20 ppm and a fragment mass tolerance of 0.1 Da. Carbamidomethylation was selected as fixed modification on Cys residues. Variable modifications selected are shown in Table S4. All *O*-linked glycopeptide sequences assigned are shown in Table S5.

Preparation of dEGF20 from bacteria

Rosetta-gami2 (DE3) *E. coli* was transformed with pET22b (+)/*dEGF20His*, and cultured in the presence of 0.5 mM IPTG at 21 °C for 2 days. The *bacterial* pellet was resuspended in

equilibration buffer (50 mM Tris-HCl, pH 8.0, 150 mM NaCl, and 10 mM imidazole). After sonication, the sample was centrifuged at 6,000 × *g* for 60 min, and the soluble fractions were filtrated with a 0.45 μm filter. The filtrate was applied to the column with Complete His Tag Purification Resin (Roche Applied Science) followed by washing with the equilibration buffer, and dEGF20 was eluted with elution buffer (50 mM Tris-HCl, pH 8.0, 150 mM NaCl, and 500 mM imidazole). The folded dEGF20 was purified using HPLC equipped with a C18 column (L-column3 C18 5 μm, 4.6 × 150 mm, Ceri). The LC gradient with 0.1% TFA as solution A and 0.1% TFA in ACN as solution B was set as follows: 20–45% B (0–10 min), 45–55% B (10–20 min), 55–90% B (20–25 min), and 90% B (25–30 min).

In vitro EOGT activity assay

For the detection of enzymatic products by HPLC, 0.2 μg of purified WT or mutant EOGT was incubated with 3 μg of dEGF20 and 1 mM UDP-GlcNAc in a 100-μl reaction buffer (100 mM Hepes, pH 7.0, and 10 mM $MnCl_2$) at 37 °C for 30 min. Control reactions were performed without the enzyme. The reaction was stopped by the addition of 900 μl of 100 mM EDTA at pH 8.2. The samples were analyzed by an HPLC system (Shimazu) equipped with a C18 column as described previously (43).

UDP-Glo glycosyltransferase assay was carried out at 37 °C in 25 μl of reaction buffer containing 100 μM UDP-GlcNAc, 50 μM dEGF20, and 0.05 μg of WT or mutated EOGT. Subsequently, 25 μl of UDP Detection Reagent containing an UDP-Glo enzyme and an ATP detection substrate was added into the reaction mixtures and incubated for 60 min at room temperature. The luminescence output was recorded utilizing a plate reader (Powerscan4, Biotech). A reaction without EOGT was used as a negative control.

Extraction of soluble and insoluble protein fractions

HEK293T cells stably expressing WT or mutant EOGT were suspended in 200 μl of TBS containing 0.1% digitonin and sonicated for 10 min on ice followed by incubation on ice for 10 min. Then, the samples were centrifuged at 2000 × *g* at 4 °C for 10 min. The supernatants containing soluble proteins were separated from the pellets. To obtain the insoluble fraction, proteins in the pellets were resuspended in 200 μl of ice-cold 1% Nonidet P-40 in TBS, vortexed for 10 s, incubated on ice for 15 min, and centrifuged at 15,000 × *g* at 4 °C for 15 min to remove the debris.

Immunostaining

Cells were fixed with 4% paraformaldehyde in PBS for 15 min and cold 100% MeOH for 5 min at room temperature. Fixed cells were permeabilized with 0.5% Triton X-100 in PBS for 15 min and blocked with blocking buffer (5% BSA in PBS) for 30 min. Immunostaining was performed as described previously (4) utilizing the primary antibodies and fluorescent dye-conjugated secondary antibodies (Table S1). The stained cells were placed on a glass slide with DAPI-Fluormount (Southern Biotech). All samples were analyzed by TiEA1R Confocal Microscopy with NIS Elements (Nikon). To simultaneously perform the phalloidin and antibody staining methods, the MeOH fixation step was omitted and Alexa Fluor 555 phalloidin (Invitrogen) was added to the secondary antibody solution at 1/1000 dilution.

For quantitative analysis of EOGT and Calnexin staining, cytoplasmic regions up to ~1 μM from cell surface and ~1 μM from nuclear envelope were defined as peripheral and perinuclear regions, respectively. Signal intensity in each cytoplasmic region was calculated using NIS elements software (Fig. S5*B*).

Data availability

Data are available by accessing JPOST at the following URL's: *N*-glycan analysis of EOGT by trypsin digestion ID: https://repository.jpostdb.org/entry/JPST000829]; *N*-glycan analysis of EOGT by chymotrypsin digestion ID: https://repository.jpostdb.org/entry/JPST000828]JPST000828; and Notch1 glycopeptide in EOGT mutant ID: https://repository.jpostdb.org/entry/JPST000786]JPST000786.

Acknowledgments—We thank the Division for Medical Research Engineering, Nagoya University Graduate School of Medicine, and Kentaro Taki for the operation of LC-MS/MS and Dr. Shogo Sawaguchi (Nagoya University) for the generation of *EOGT*-deficient HEK293T cells.

Author contributions—S. M. D. A., Y. Tsukamoto, and Y. S. data curation; S. M. D. A., Y. Tsukamoto, and M. O. formal analysis; S. M. D. A. investigation; S. M. D. A., Y. Tsukamoto, M. O., and Y. S. methodology; S. M. D. A. and T. O. writing-original draft; S. M. D. A., M. O., H. T., and T. O. writing-review and editing; M. O., K. I., Y. Tashima, H. T., and T. O. funding acquisition; K. I., H. T., and T. O. supervision; Y. Tashima resources; T. O. conceptualization; T. O. project administration.

Funding and additional information—This work was supported by JSPS KAKENHI Grant JP19H03416 (to T. O.), JP19H03176 (to H. T.), and JP19K16073 (to M. O.), and grants from the Mitsubishi Foundation (to T. O.), the Japan Foundation for Applied Enzymology (to T. O.), Takeda Science Foundation (to M. O. and H. T.), The Hori Sciences and Arts foundation (M. O.), and Foundation for Promotion of Cancer Research (M. O.).

Conflict of interest—The authors declare that they have no conflicts of interest regarding the content of this article.

Abbreviations—The abbreviations used are: EGF, epidermal growth factor; ACN, acetonitrile; ConA, concanavalin A; EIC, extracted ion chromatogram; Endo H, endoglycosidase H; ER, endoplasmic reticulum; IPTG, isopropyl 1-thio-β-D-galactopyranoside; PNGase F, peptide:*N*-glycosidase F; IRES, internal ribosome entry site; HUVEC, human umbilical vein endothelial cell; TM, transmembrane; GM3, *N*-acetylneuraminylgalactosylceramide; PEI, polyethyleneimine; ITS, insulin-transferrin-selenium; PVDF, polyvinylidene difluoride; HRP, horseradish peroxidase; EOGT, O-GlcNAc transferase; TBS, Tris-buffered saline; Th, thomson.

References

1. Matsuura, A., Ito, M., Sakaidani, Y., Kondo, T., Murakami, K., Furukawa, K., Nadano, D., Matsuda, T., and Okajima, T. (2008) *O*-Linked *N*-acetylglucosamine is present on the extracellular domain of notch receptors. *J. Biol. Chem.* **283,** 35486–35495 CrossRef Medline
2. Sakaidani, Y., Ichiyanagi, N., Saito, C., Nomura, T., Ito, M., Nishio, Y., Nadano, D., Matsuda, T., Furukawa, K., and Okajima, T. (2012) *O*-Linked-*N*-acetylglucosamine modification of mammalian Notch receptors by an atypical *O*-GlcNAc transferase Eogt1. *Biochem. Biophys. Res. Commun.* **419,** 14–19 CrossRef Medline
3. Tashima, Y., and Stanley, P. (2014) Antibodies that detect *O*-linked β-D-*N*-acetylglucosamine on the extracellular domain of cell surface glycoproteins. *J. Biol. Chem.* **289,** 11132–11142 CrossRef Medline
4. Sawaguchi, S., Varshney, S., Ogawa, M., Sakaidani, Y., Yagi, H., Takeshita, K., Murohara, T., Kato, K., Sundaram, S., Stanley, P., and Okajima, T. (2017) *O*-GlcNAc on NOTCH1 EGF repeats regulates ligand-induced Notch signaling and vascular development in mammals. *Elife* **6,** CrossRef
5. Shaheen, R., Aglan, M., Keppler-Noreuil, K., Faqeih, E., Ansari, S., Horton, K., Ashour, A., Zaki, M. S., Al-Zahrani, F., Cueto-González, A. M., Abdel-Salam, G., Temtamy, S., and Alkuraya, F. S. (2013) Mutations in EOGT confirm the genetic heterogeneity of autosomal-recessive Adams-Oliver syndrome. *Am. J. Hum. Genet.* **92,** 598–604 CrossRef Medline
6. Cohen, I., Silberstein, E., Perez, Y., Landau, D., Elbedour, K., Langer, Y., Kadir, R., Volodarsky, M., Sivan, S., Narkis, G., and Birk, O. S. (2014) Autosomal recessive Adams-Oliver syndrome caused by homozygous mutation in EOGT, encoding an EGF domain-specific *O*-GlcNAc transferase. *Eur. J. Hum. Genet.* **22,** 374–378 CrossRef Medline
7. Ogawa, M., Sawaguchi, S., Kawai, T., Nadano, D., Matsuda, T., Yagi, H., Kato, K., Furukawa, K., and Okajima, T. (2015) Impaired *O*-linked *N*-acetylglucosaminylation in the endoplasmic reticulum by mutated epidermal growth factor (EGF) domain-specific *O*-linked *N*-acetylglucosamine transferase found in Adams-Oliver syndrome. *J. Biol. Chem.* **290,** 2137–2149 CrossRef Medline
8. Allam, H., Johnson, B. P., Zhang, M., Lu, Z., Cannon, M. J., and Abbott, K. L. (2017) The glycosyltransferase GnT-III activates Notch signaling and drives stem cell expansion to promote the growth and invasion of ovarian cancer. *J. Biol. Chem.* **292,** 16351–16359 CrossRef Medline
9. Wang, Y., Shao, L., Shi, S., Harris, R. J., Spellman, M. W., Stanley, P., and Haltiwanger, R. S. (2001) Modification of epidermal growth factor-like repeats with *O*-fucose: molecular cloning and expression of a novel GDP-fucose protein *O*-fucosyltransferase. *J. Biol. Chem.* **276,** 40338–40345 CrossRef Medline
10. Loriol, C., Audfray, A., Dupuy, F., Germot, A., and Maftah, A. (2007) The two *N*-glycans present on bovine Pofut1 are differently involved in its solubility and activity. *FEBS J.* **274,** 1202–1211 CrossRef Medline
11. Takeuchi, H., Wong, D., Schneider, M., Freeze, H. H., Takeuchi, M., Berardinelli, S. J., Ito, A., Lee, H., Nelson, S. F., and Haltiwanger, R. S. (2018) Variant in human POFUT1 reduces enzymatic activity and likely causes a recessive microcephaly, global developmental delay with cardiac and vascular features. *Glycobiology* **28,** 276–283 CrossRef Medline
12. Isono, T. (2011) *O*-GlcNAc-specific antibody CTD110.6 cross-reacts with N-GlcNAc2-modified proteins induced under glucose deprivation. *PLoS ONE* **6,** e18959 CrossRef Medline
13. Ogawa, M., Nakamura, N., Nakayama, Y., Kurosaka, A., Manya, H., Kanagawa, M., Endo, T., Furukawa, K., and Okajima, T. (2013) GTDC2 modifies *O*-mannosylated α-dystroglycan in the endoplasmic reticulum to generate *N*-acetyl glucosamine epitopes reactive with CTD110.6 antibody. *Biochem. Biophys. Res. Commun.* **440,** 88–93 CrossRef Medline
14. Ogawa, M., Senoo, Y., Ikeda, K., Takeuchi, H., and Okajima, T. (2018) Structural divergence in *O*-GlcNAc glycans displayed on epidermal growth factor-like repeats of mammalian Notch1. *Molecules* **23,** 1745 CrossRef
15. Acar, M., Jafar-Nejad, H., Takeuchi, H., Rajan, A., Ibrani, D., Rana, N. A., Pan, H., Haltiwanger, R. S., and Bellen, H. J. (2008) Rumi is a CAP10 domain glycosyltransferase that modifies Notch and is required for Notch signaling. *Cell* **132,** 247–258 CrossRef Medline
16. Takeuchi, H., Kantharia, J., Sethi, M. K., Bakker, H., and Haltiwanger, R. S. (2012) Site-specific *O*-glucosylation of the epidermal growth factor-like (EGF) repeats of notch: efficiency of glycosylation is affected by proper folding and amino acid sequence of individual EGF repeats. *J. Biol. Chem.* **287,** 33934–33944 CrossRef Medline
17. Gao, G., Zhu, C., Liu, E., and Nabi, I. R. (2019) Reticulon and CLIMP-63 regulate nanodomain organization of peripheral ER tubules. *PLos Biol.* **17,** e3000355 CrossRef Medline
18. Nixon-Abell, J., Obara, C. J., Weigel, A. V., Li, D., Legant, W. R., Xu, C. S., Pasolli, H. A., Harvey, K., Hess, H. F., Betzig, E., Blackstone, C., and Lippincott-Schwartz, J. (2016) Increased spatiotemporal resolution reveals highly dynamic dense tubular matrices in the peripheral ER. *Science* **354,** aaf3928–aaf3928 CrossRef Medline
19. Varki, A. (2017) Biological roles of glycans. *Glycobiology* **27,** 3–49 CrossRef Medline
20. Ioffe, E., and Stanley, P. (1994) Mice lacking *N*-acetylglucosaminyltransferase I activity die at mid-gestation, revealing an essential role for complex or hybrid N-linked carbohydrates. *Proc. Natl. Acad. Sci. U.S.A.* **91,** 728–732 CrossRef Medline
21. Schwarz, F., and Aebi, M. (2011) Mechanisms and principles of *N*-linked protein glycosylation. *Curr. Opin. Struct. Biol.* **21,** 576–582 CrossRef Medline
22. Lopez-Sambrooks, C., Shrimal, S., Khodier, C., Flaherty, D. P., Rinis, N., Charest, J. C., Gao, N., Zhao, P., Wells, L., Lewis, T. A., Lehrman, M. A., Gilmore, R., Golden, J. E., and Contessa, J. N. (2016) Oligosaccharyltransferase inhibition induces senescence in RTK-driven tumor cells. *Nat. Chem. Biol.* **12,** 1023–1030 CrossRef Medline
23. Contessa, J. N., Bhojani, M. S., Freeze, H. H., Ross, B. D., Rehemtulla, A., and Lawrence, T. S. (2010) Molecular imaging of *N*-linked glycosylation suggests glycan biosynthesis is a novel target for cancer therapy. *Clin. Cancer Res.* **16,** 3205–3214 CrossRef Medline
24. Liu, Y., Ren, S., Xie, L., Cui, C., Xing, Y., Liu, C., Cao, B., Yang, F., Li, Y., Chen, X., Wei, Y., Lu, H., and Jiang, J. (2015) Mutation of *N*-linked glycosylation at Asn548 in CD133 decreases its ability to promote hepatoma cell growth. *Oncotarget* **6,** 20650–20660 CrossRef Medline
25. Fuster, M. M., and Esko, J. D. (2005) The sweet and sour of cancer: glycans as novel therapeutic targets. *Nat. Rev. Cancer* **5,** 526–542 CrossRef Medline
26. Taniguchi, N., and Kizuka, Y. (2015) Glycans and cancer: role of *N*-glycans in cancer biomarker, progression and metastasis, and therapeutics. *Adv. Cancer Res.* **126,** 11–51 CrossRef Medline
27. Shrimal, S., Trueman, S. F., and Gilmore, R. (2013) Extreme C-terminal sites are posttranslocationally glycosylated by the STT3B isoform of the OST. *J. Cell Biol.* **201,** 81–95 CrossRef Medline
28. Wells, L., Whelan, S. A., and Hart, G. W. (2003) *O*-GlcNAc: a regulatory post-translational modification. *Biochem. Biophys. Res. Commun.* **302,** 435–441 CrossRef Medline
29. Fast, D. G., Jamieson, J. C., and McCaffrey, G. (1993) The role of the carbohydrate chains of Galβ-1,4-GlcNAc α2,6-sialyltransferase for enzyme activity. *Biochim. Biophys. Acta* **1202,** 325–330 CrossRef Medline
30. Haraguchi, M., Yamashiro, S., Furukawa, K., Takamiya, K., Shiku, H., and Furukawa, K. (1995) The effects of the site-directed removal of *N*-glycosylation sites from β-1,4-*N*-acetylgalactosaminyltransferase on its function. *Biochem. J.* **312,** 273–280 CrossRef Medline
31. Nagai, K., Ihara, Y., Wada, Y., and Taniguchi, N. (1997) *N*-Glycosylation is requisite for the enzyme activity and Golgi retention of *N*-acetylglucosaminyltransferase III. *Glycobiology* **7,** 769–776 CrossRef Medline
32. Martina, J. A., Daniotti, J. L., and Maccioni, H. J. (2000) GM1 synthase depends on N-glycosylation for enzyme activity and trafficking to the Golgi complex. *Neurochem. Res.* **25,** 725–731 CrossRef Medline
33. Uemura, S., Kurose, T., Suzuki, T., Yoshida, S., Ito, M., Saito, M., Horiuchi, M., Inagaki, F., Igarashi, Y., and Inokuchi, J. (2006) Substitution of the *N*-glycan function in glycosyltransferases by specific amino acids: ST3Gal-V as a model enzyme. *Glycobiology* **16,** 258–270 CrossRef Medline
34. Martina, J. A., Daniotti, J. L., and Maccioni, H. J. (1998) Influence of *N*-glycosylation and *N*-glycan trimming on the activity and intracellular traffic of GD3 synthase. *J. Biol. Chem.* **273,** 3725–3731 CrossRef Medline

35. Manya, H., Akasaka-Manya, K., Nakajima, A., Kawakita, M., and Endo, T. (2010) Role of *N*-glycans in maintaining the activity of protein *O*-mannosyltransferases POMT1 and POMT2. *J. Biochem.* **147,** 337–344 CrossRef Medline
36. Hebert, D. N., Lamriben, L., Powers, E. T., and Kelly, J. W. (2014) The intrinsic and extrinsic effects of *N*-linked glycans on glycoproteostasis. *Nat. Chem. Biol.* **10,** 902–910 CrossRef Medline
37. St-Pierre, P., Dang, T., Joshi, B., and Nabi, I. R. (2012) Peripheral endoplasmic reticulum localization of the Gp78 ubiquitin ligase activity. *J. Cell Sci.* **125,** 1727–1737 CrossRef Medline
38. Holcman, D., Parutto, P., Chambers, J. E., Fantham, M., Young, L. J., Marciniak, S. J., Kaminski, C. F., Ron, D., and Avezov, E. (2018) Single particle trajectories reveal active endoplasmic reticulum luminal flow. *Nat. Cell Biol.* **20,** 1118–1125 CrossRef Medline
39. Ellgaard, L., McCaul, N., Chatsisvili, A., and Braakman, I. (2016) Co- and post-translational protein folding in the ER. *Traffic* **17,** 615–638 CrossRef Medline
40. Takeuchi, H., Schneider, M., Williamson, D. B., Ito, A., Takeuchi, M., Handford, P. A., and Haltiwanger, R. S. (2018) Two novel protein *O*-glucosyltransferases that modify sites distinct from POGLUT1 and affect Notch trafficking and signaling. *Proc. Natl. Acad. Sci. U.S.A.* **115,** E8395–E8402 CrossRef Medline
41. Hou, X., Tashima, Y., and Stanley, P. (2012) Galactose differentially modulates lunatic and manic fringe effects on Delta1-induced NOTCH signaling. *J. Biol. Chem.* **287,** 474–483 CrossRef Medline
42. Liu, G., Cheng, K., Lo, C. Y., Li, J., Qu, J., and Neelamegham, S. (2017) A comprehensive, open-source platform for mass spectrometry-based glycoproteomics data analysis. *Mol. Cell. Proteomics* **16,** 2032–2047 CrossRef Medline
43. Ogawa, M., Tashima, Y., Sakaguchi, Y., Takeuchi, H., and Okajima, T. (2020) Contribution of extracellular O-GlcNAc to the stability of folded epidermal growth factor-like domains and Notch1 trafficking. *Biochem. Biophys. Res. Commun.* **526,** 184–190 CrossRef Medline